Molecular dynamics simulation of compression-induced solid-to-solid phase transitions in colloidal monolayers

Jizhong Sun and T. Stirner*
Department of Chemistry, University of Hull, Hull HU6 7RX, United Kingdom
(Received 22 January 2003; published 19 May 2003)

The compression of two-dimensional colloidal monolayers, consisting of polystyrene particles trapped at an oil-water interface and interacting via dipole-dipole potentials, is investigated by the molecular dynamics technique. In particular, the pair correlation function and global orientational order parameter of the monolayers are calculated as a function of the particle coverage. The simulation results exhibit a sequence of hexagonal-to-rhombohedral-to-hexagonal phase transitions of the monolayers under anisotropic compression. The influence of defects in the monolayers on the solid-to-solid phase transitions is also examined. The simulations show that the stability of the rhombohedral phase is relatively sensitive to lattice defects, while, under the same conditions, the hexagonal phase is very stable. Finally, the simulation results are compared with recent experimental observations, and the implications of the present computer simulations for diffusion mechanisms and protein folding studies are discussed briefly.

DOI: 10.1103/PhysRevE.67.051107 PACS number(s): 64.60.−i, 64.70.Kb

I. INTRODUCTION

Colloidal particles occur widely in nature and have many practical applications in widely diversed technological fields, such as inks, detergents, paints, oil recovery, paper and food manufacture [1–3]. Recently, it has been shown that the presence of colloidal particles at interfaces can drastically affect the physical properties of the interface, such as the stability of emulsions and foams [4–6]. In addition to the technological importance, monolayers of charged colloidal particles trapped at an interface (such as air-water or oil-water) have been proposed as analogs to two-dimensional condensed-phase atomic systems. Here, the main interest stems from their ability to replicate melting and crystallization phenomena in two dimensions [7–12].

Since Pieranski [13] first found that polystyrene particles are trapped at the air-water interface and form two-dimensional triangular lattices, much attention has been drawn to the determination of their physical and thermodynamical properties. Highly uniform microspheres (≈ 0.1–5 μm in diameter) are commercially available. These particles are large enough to be observable using optical microscopy, and their positions and trajectories can therefore be easily monitored. In addition, the interaction between these particles is relatively simple, which makes these systems very attractive to theoretical and experimental studies.

In the 1970s, Kosterlitz and Thouless [14], Halperin and Nelson [15], and Young [16] (KTHNY) put forward a theory of defect-mediated melting in which it was proposed that the dissociation of dislocation pairs causes the two-dimensional solid to melt via sequential, continuous (in contrast to first-order) phase transitions. Subsequently, many computer simulation studies, employing the molecular dynamics or Monte Carlo techniques, were carried out, with some groups [8,12] claiming support for the KTHNY theory, while others [7,9,11] found results that were not consistent with the predictions of the KTHNY theory. In these investigations, the particles trapped at a two-dimensional interface were represented by different interaction potentials. For instance, Kalia and Vashishta [7] used a dipole-dipole interaction potential, while Frenkel and McTague [8] and Toxvaerd [9] employed the Lennard-Jones potential to model the particle monolayers. Zangi and Rice [11] used another interaction potential designed to have the features inferred by Marcus and Rice [17]. The application of these different interaction potentials may, in part, be the reason why a consistent conclusion with regard to the validity of the KTHNY theory has not yet been drawn [12]. In the experimental study of Armstrong *et al.* [10], the system of polystyrene particles of 2.88 μm diameter at the air-water interface showed evidence of defect-mediated melting and of an intermediate hexatic phase, while melting in their 1.01-μm system appeared to proceed by a weak first-order transition. This would imply that the difference in melting behavior between the two samples reflects differences in defect core creation energies which can be traced to the sphere size.

In spite of these controversies, there is no doubt that defects will play an important role in the physics of phase transitions. Recently, Aveyard *et al.* [18] presented detailed experimental results on the structural variation of hexagonal particle monolayers under compression at air-water and oil-water interfaces. An interesting result of this work was the observed anisotropic reduction of the lattice constants of the monolayers under compression, i.e., a hexagonal-to-rhombohedral phase transition. In the present study, we are concerned with a theoretical model of the compression of such two-dimensional particle monolayers at the oil-water interface. For this purpose, the molecular dynamics (MD) technique was employed in the computer simulations. The primary aims are to investigate the conditions for the occurrence of solid-to-solid phase transitions, and to establish the role that defects play in the structural stability of the monolayers. As will become clear in the bulk of the paper, this also has important implications for diffusion mechanisms in

*Email address: t.stirner@hull.ac.uk

solids and for the study of the surface activity of antibody monolayers.

II. COMPUTER SIMULATION DETAILS

In our earlier work [19] we have described an MD model to simulate the compression of monolayers of polystyrene particles at an oil-water interface in detail. Possible interaction mechanisms between the particles, i.e., charge-charge, charge-dipole, and dipole-dipole interactions, were discussed. Attention was then focused on a calculation of the surface pressure of the monolayers, and the results were compared with the experimental measurements of Aveyard *et al.* [18]. These calculations showed that, for certain experimental conditions [18], there is a significant contribution from charge-charge interactions for large particle separations. However, it was also demonstrated [19] that the short-range particle interactions can be very well approximated by dipole-dipole interactions. Hence, in the present work, we will focus on dipole-dipole interactions only.

In Ref. [19], we have derived an expression for the interaction energy E between two parallel point dipoles of moment P. Each dipole was assumed to be located on a particle of radius R, with the center-to-center separation between the particles being denoted by r. The final equation is given by

$$E=\frac{P^2}{16\pi\varepsilon r R^2}[2\ln r-\ln(r+2R)-\ln(r-2R)], \qquad (1)$$

where ε is the permittivity of the dielectric medium (in the present case oil with a value of $\varepsilon_r=2$). The interaction energy in Eq. (1) behaves as r^{-3} for large r and is employed in the present MD simulations of the colloidal monolayers at the oil-water interface. In order to make the water–oil–particle-monolayer system tractable on a computer, only the interactions between the colloidal particles are evaluated in the MD calculations, while the oil phase is simulated by its static dielectric constant in the particle interaction energies (only the interactions between the particles through the oil phase are considered since the relative permittivity of water is 78 at room temperature, compared with a relative permittivity of oil of 2). The oil-water interface is assumed to be planar, since we know from the experiments [18] that the colloidal particles are trapped in a deep surface potential well, and that monolayer folding and/or corrugations only occur above the monolayer collapse pressure. In the present study, the particles are large enough (particle radius $R=1.3\ \mu$m) not to be affected by the Brownian motion. The MD simulations of the monolayer compression are performed for $N=1000$ colloidal particles in a rectangular cell with periodic boundary conditions. Convergence tests for this system (i.e., to eliminate finite-size effects) were published previously in Ref. [19]. Initially, the particles are distributed randomly within the simulation cell. Similarly, the particle velocities are sampled randomly from a Boltzmann distribution [20]. The ratio of the potential to kinetic energy of the particles was chosen to be relatively large (i.e., 3.77×10^6), in order to obtain acceptable run times of the MD computer program on the machine employed for the calculations (we will come back to this point in the next section). The cell area A is determined by the particle coverage (i.e., $A=\pi R^2 N/\text{coverage}$). The system is then allowed to relax into a local equilibrium configuration before the monolayer compression begins. (This procedure is analogous to the experiments, where the monolayers were left for $\approx$15 min–1 h prior to the start of the measurements [18,21].) In the experiments [18], the compression of the monolayers was anisotropic. Hence, in the MD simulations, the distance between two parallel sides of the simulation cell is reduced slowly, which corresponds to an increase in the value of the coverage. The coverage is incremented in steps of 0.05, which takes typically 10 000 time steps, with a time step of 40 ns. The system is then equilibrated for $\approx$5000 time steps at each value of the coverage.

In order to characterize the structure of the colloidal monolayers quantitatively, we have evaluated the pair correlation function [20]

$$g(r)=\frac{A}{N^2}\left\langle\sum_{i=1}^{N}\sum_{j\neq i}^{N}\delta(\mathbf{r}-\mathbf{r}_{ij})\right\rangle \qquad (2)$$

and the global orientational order parameter [11]

$$\Phi_6=\frac{1}{N}\sum_{i=1}^{N}\frac{1}{n_i}\sum_{j=1}^{n_i}e^{i6\Theta_{ij}}, \qquad (3)$$

where A is the area of the simulation cell, N is the number of particles, n_i is the number of nearest neighbors to particle i, $\mathbf{r}_{ij}(=\mathbf{r}_i-\mathbf{r}_j)$ is the separation between particles i and j, and Θ_{ij} is the angle between $\mathbf{r}_{ij}$ and an arbitrary fixed axis. Equation (2) gives the probability of finding a pair of particles a distance r apart, relative to the probability for a completely random distribution at the same particle density. The quantity $|\Phi_6|^2$ is very sensitive to the structural order of the system. When the monolayer is in a random (''fluidlike'') phase and there is no structural order, the value of $|\Phi_6|^2 \ll 1$. On the other hand, $|\Phi_6|^2$ takes a value close to 1, when the colloidal particles form a crystal with hexagonal order.

III. RESULTS AND DISCUSSION

A. Compression of particle monolayers

The particle configuration after the initial equilibration phase at a coverage of 0.3 is shown in Fig. 1(a). The corresponding pair correlation function is shown in Fig. 2. As can be seen, there is good local, hexagonal order in the monolayer (the ratios of the lattice constants for the first four peaks in Fig. 2 are almost exactly $1:\sqrt{3}:2:\sqrt{7}$ corresponding to perfect hexagonal packing). However, the monolayer exhibits a number of domains of different lattice orientation, with lattice defects occurring predominantly at the grain boundaries. Here, some particles have five and some have seven nearest neighbors. This is shown schematically in Fig. 1(b), which displays the same configuration as Fig. 1(a) except that the particles with five nearest neighbors are labeled *B*, the particles with seven nearest neighbors are labeled *N*, while the particles with six nearest neighbors are labeled *C*.

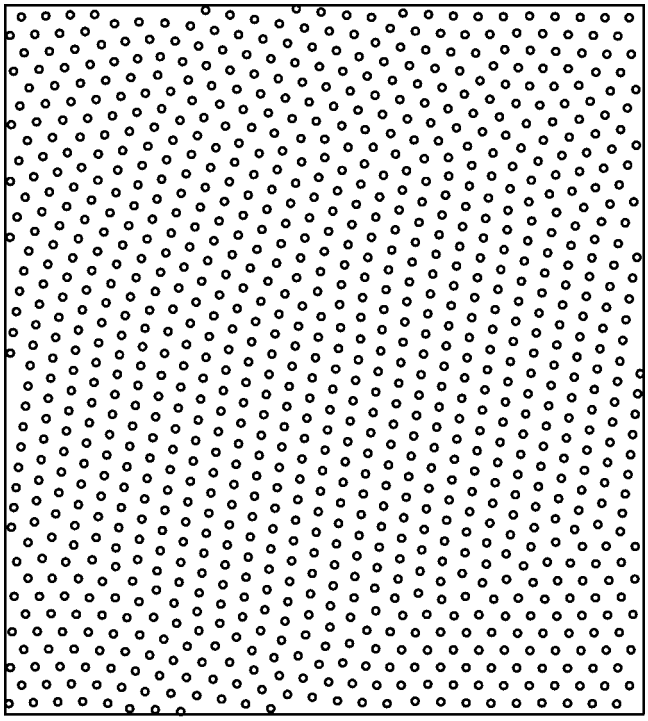

(a)

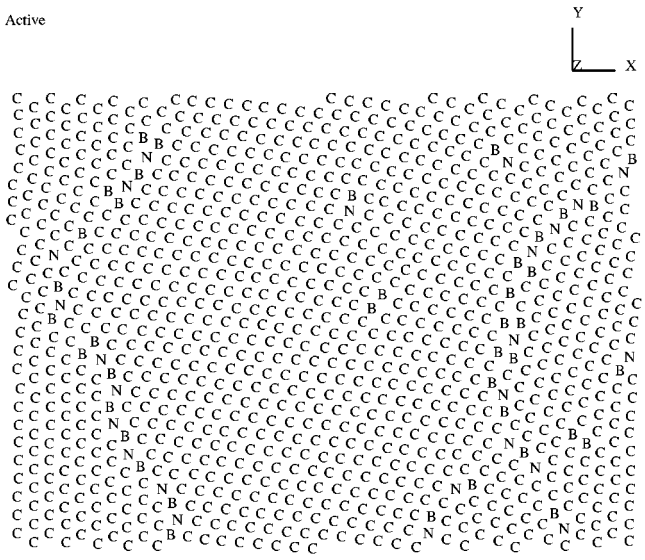

(b)

FIG. 1. (a) Initial (relaxed) configuration of the particle monolayer at the oil-water interface (particle radius $R=1.3\ \mu$m; coverage=0.3). (b) Schematic diagram of the coordination numbers of the particles corresponding to the configuration in (a). B, C, and N denote particles having five, six, and seven nearest neighbors, respectively.

It is interesting to note that most defects occur in pairs (e.g., pairs of *B*'s usually denote edge dislocations). This indicates that defect pairs have a lower energy than two isolated defects. Similarly, some particles that do have six nearest neighbors do not form congruent hexagons with their neighboring unit cells. In addition, the largest, central domain contains several dislocations (clearly visible on inspection of Fig. 1 at a very low angle). Both, the formation of a domain structure and edge dislocations were also observed in the experiments of Aveyard *et al.* (see, e.g., Fig. 3(a) of Ref. 21 and Fig. 7(b) of Ref. [18]). However, despite these defects, the corresponding pair correlation function (Fig. 2) shows distinct, sharp peaks at the lattice constants of a hexagonal monolayer.

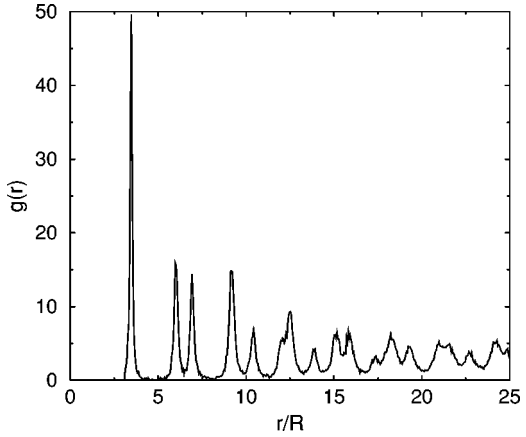

FIG. 2. Pair correlation function for the initial configuration of the monolayer shown in Fig. 1.

Figure 3 shows the pair correlation function for the case where the monolayer of Fig. 1 has been compressed to a coverage of 0.35. The pair correlation function for this coverage is similar to that shown in Fig. 2, except that the main peaks split into two smaller peaks. This splitting arises from the anisotropic compression of the monolayer, which, in turn, leads to a rhombohedral lattice structure. Such a compression-induced hexagonal-to-rhombohedral phase transition was also observed experimentally by Aveyard *et al.* [18]. If now the compression of the monolayer in the rhombohedral phase is continued, then, at a coverage of ≈ 0.42, a phase transition back to hexagonal packing occurs. This is illustrated by the pair correlation function shown in Fig. 4 corresponding to a coverage of 0.45. As can be seen, the pair correlation function displays single, narrow peaks resulting from a very good hexagonal ordering of the mono-

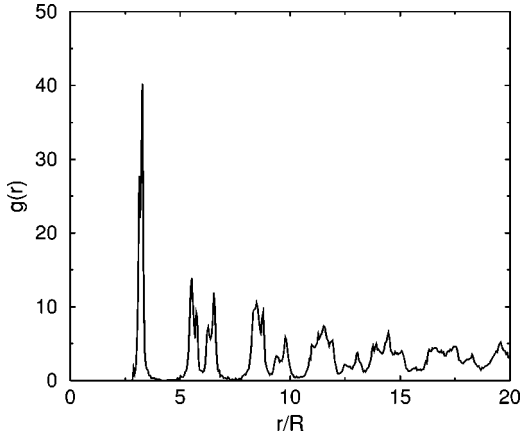

FIG. 3. Pair correlation function of the monolayer shown in Fig. 1 compressed to the particle coverage of 0.35.

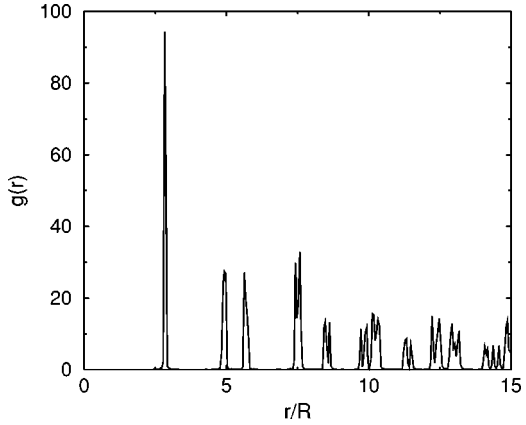

FIG. 4. Pair correlation function of the monolayer shown in Fig. 1 compressed to the particle coverage of 0.45.

layer. In addition, all grain boundaries have disappeared and the monolayer is almost defect free.

The process described immediately above (of a hexagonal-to-rhombohedral-to-hexagonal phase transition) is then repeated for increasing coverages. This is illustrated in Fig. 5, which shows the height of the first peak of the pair correlation function (corresponding to the number and distribution of nearest-neighbor particles) as a function of coverage. Visible in this figure are two distinct maxima (at coverages of ≈ 0.45 and 0.55) corresponding to hexagonal packing. The third maximum (at the initial coverage of 0.3) is much reduced in height compared with the other two maxima, due to the large number of defects present in the monolayer at this coverage. For intermediate coverages (between two maxima), the packing is rhombohedral.

The percentage of defects in the monolayer (defined as the ratio of the number of particles having either five or seven nearest neighbors to the total number of particles) as a function of coverage is shown in Fig. 6. As mentioned above, the number of defects decreases dramatically at the first rhombohedral-to-hexagonal phase transition point (at a coverage of ≈ 0.42). In contrast to this, the second compression-induced rhombohedral-to-hexagonal phase transition (at a

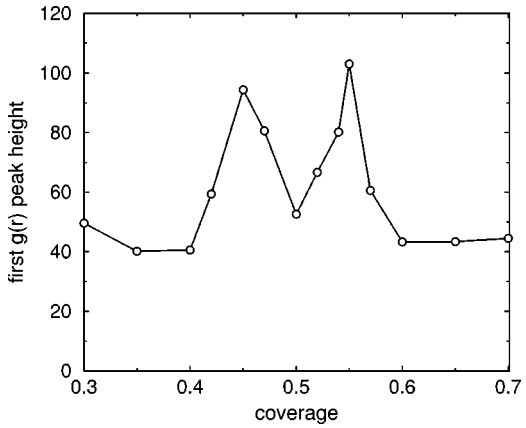

FIG. 5. Height of the first peak of the pair correlation function corresponding to the monolayer shown in Fig. 1 as a function of the particle coverage (representing the compression of the monolayer).

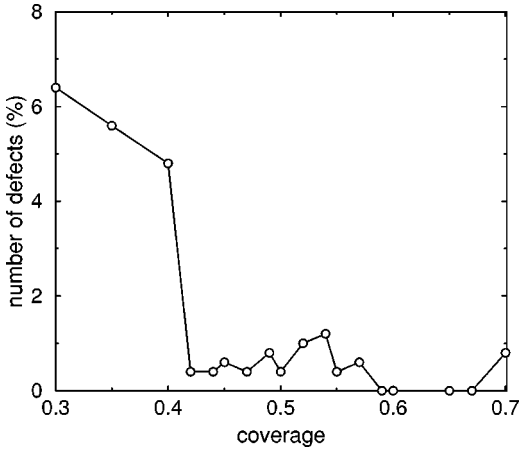

FIG. 6. Percentage of defects (particles having either five or seven nearest neighbors) as a function of coverage for the monolayer of Fig. 1.

coverage of ≈ 0.55) gives rise to only a slight decrease in the number of defects, mainly because the intermediate rhombohedral phase is already of very high structural quality. We note here that the absolute magnitude of the percentage of defects is somewhat arbitrary since it depends on the exact initial particle configuration (which is chosen randomly in the present calculations). However, the occurrence of two consecutive hexagonal-to-rhombohedral-to-hexagonal phase transitions is independent of the exact choice of initial configuration. Similarly, the global orientational order parameter for the monolayer, shown in Fig. 7, increases to a value of $|\Phi_6|^2 \approx 0.97$ beyond the first rhombohedral-to-hexagonal phase transition point, which reflects the good, long-range orientational order of the compressed lattice structure. The magnitude of $|\Phi_6|^2$ is mainly affected by two structural characteristics of the monolayer. First, the number of lattice defects, i.e., a larger number of defects gives rise to a smaller value of $|\Phi_6|^2$ since defects disrupt the order of the triangular lattice. Second, the deformation of hexagons, i.e., even for a monolayer without defects, the deformation of the hexagons gives rise to a decrease in the value of $|\Phi_6|^2$. For example, the low values of $|\Phi_6|^2$ in Fig. 7 for coverages

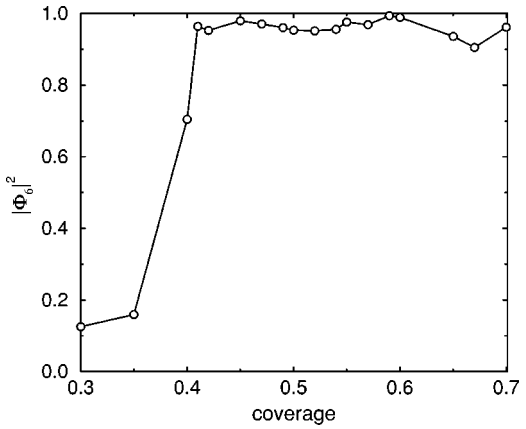

FIG. 7. Modulus squared of the global orientational order parameter versus particles coverage for the monolayer of Fig. 1.

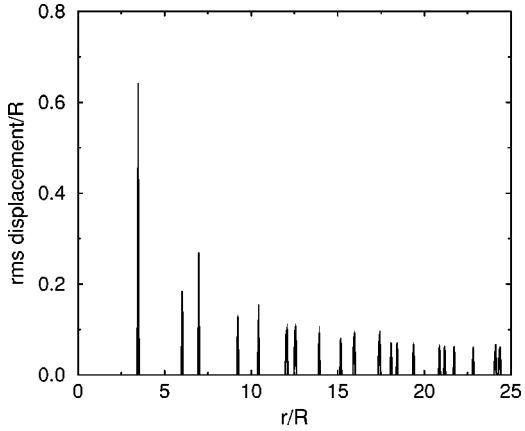

FIG. 8. Root-mean-square displacement of the particles adjacent to the vacancy (coverage=0.3). The first peak corresponds to the displacement of the nearest neighbors, the second peak to the next-nearest neighbors, etc.

below ≈ 0.4 result mainly from a high percentage of defects (cf. Fig. 6), whereas the reduction of $|\Phi_6|^2$ for coverages between 0.6 and 0.67 arises mainly from the deformation of the triangular lattice under compression. It is interesting to note that the behavior shown in Figs. 6 and 7 is very similar to the liquid-to-hexatic phase transition observed in the MD simulations of Zangi and Rice [11] and Terao and Nakayama [12].

B. Schottky defects

We will now examine the influence of lattice imperfections on the stability of the monolayers in more detail. For this purpose, we have introduced a Schottky defect by removing a single particle from an otherwise perfect monolayer. The vacancy is created near the center of the simulation cell and the remaining particles are then allowed to relax into the nearest local equilibrium configuration. For a hexagonal lattice at a particle coverage of 0.3 we find that the creation of a vacancy does not impede the stability of the monolayer. The only effect of the vacancy is the displacement of neighboring particles in the direction of the defect. This is illustrated in Fig. 8, which shows the root-mean-square displacement of the particles adjacent to the vacancy. As can be seen, the displacement, in particular of the nearest neighbors, is significant (i.e., over 60% of the particle radius). However, the displacement of next-nearest neighbors, etc., is much smaller and decreases rapidly as their distance from the vacancy increases. This behavior was also found in the theoretical studies of Fisher *et al.* [22], Cockayne and Elser [23] and Frey *et al.* [24], and was recently observed experimentally by Pertsinidis and Ling [25], who used an optical tweezer method to create a vacancy in a monolayer of 0.36-μm diameter polystyrene-sulphate microspheres confined between two fused-silica substrates separated by ≈ 2 μm.

In stark contrast to this, we find that, on repeating the above procedure for a monolayer which is anisotropically compressed to the coverage of 0.35, the whole lattice rearranges such as to expel the vacancy from the simulation cell.

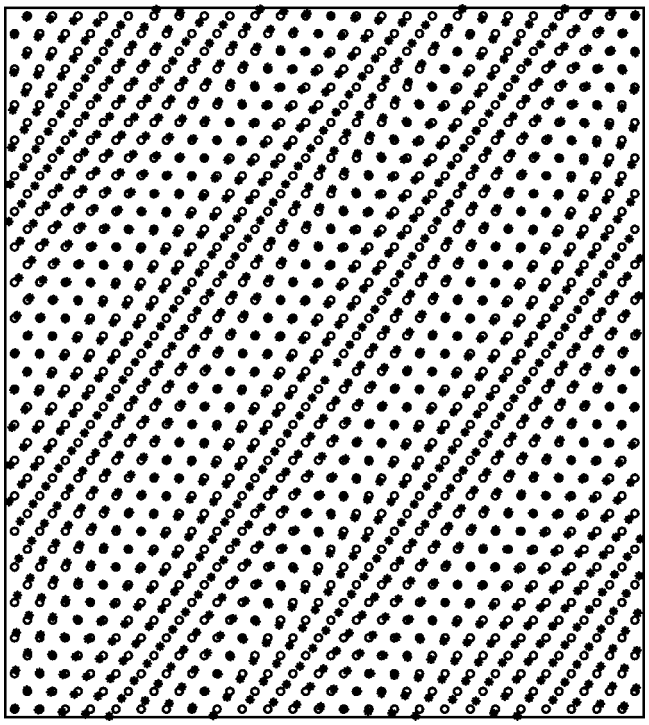

FIG. 9. Configurations of the monolayer at the coverage of 0.35. The initial configuration of the monolayer (empty circles) was obtained by compressing a perfect hexagonal monolayer (of coverage =0.3) anisotropically and then removing a particle. The final configuration, obtained after isothermal relaxation, is represented by stars.

The initial and final configurations for this scenario are shown in Fig. 9 (where the empty circles represent the initial configuration and the stars the final, energy-minimized configuration). The corresponding pair correlation functions are shown in Fig. 10. As can be seen, both the initial [Fig. 10(a)] and the final [Fig. 10(b)] configurations are rhombohedrally packed (cf. Fig. 3). However, the relaxation of this monolayer (i.e., Fig. 9) leads to a reduction of the potential energy by 0.5%, while the relaxation of the monolayer corresponding to Fig. 8 (for a coverage of 0.3) leads to a potential energy reduction by only 0.04% (although its total potential energy is, of course, lower).

The MD runs for higher particle coverages show similar results. In general, if a configuration is initially close to hexagonal packing, only the nearest neighbors of the vacancy relax, whereas if a configuration is initially in rhombohedral packing, the monolayer rearranges completely in order to expel the vacancy. For example, if the monolayer at the coverage of 0.35 (already in rhombohedral packing) is further compressed to the coverage of 0.4, the monolayer restores close to hexagonal packing during the compression. If then a vacancy is created and the monolayer is allowed to relax isothermally, only the particles in the vicinity of the vacancy will relax. This is shown in Fig. 11 (where again the empty circles represent the initial configuration and the stars represent the final configuration), although, as can be seen, the displacement of these particles is quite large and extensive. Furthermore, it is remarkable how groups of particles seem

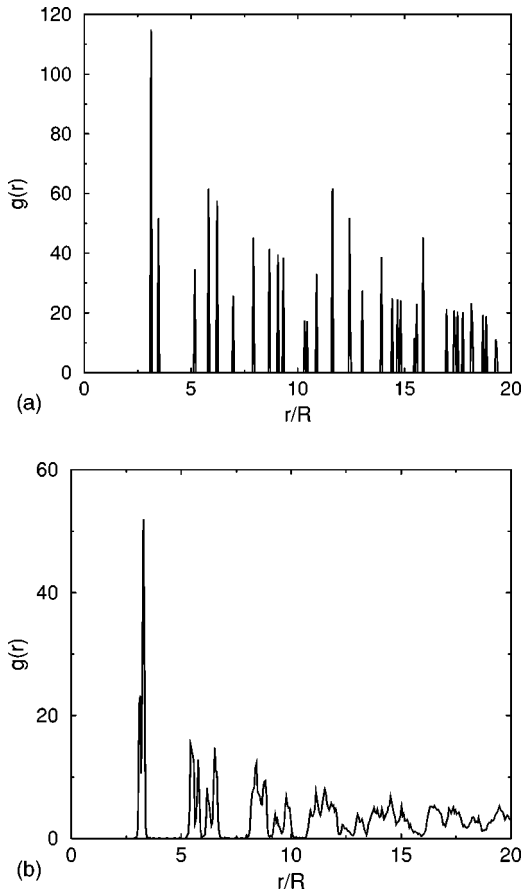

FIG. 10. Pair correlation functions of the monolayers shown in Fig. 9 (a) before and (b) after the isothermal relaxation.

to move collectively along certain lattice orientations in Fig. 11. Fundamentally, this behavior is, of course, due to the fact that for the present system, hexagonal packing is energetically favorable in comparison with rhombohedral packing. Anisotropic compression necessarily leads to rhombohedral packing, after which, in general, the system attempts to restore to hexagonal packing (or at least to a configuration that is close to hexagonal packing). However, for the transition from rhombohedral to hexagonal packing to occur, there is an energy barrier to overcome. Arising from the conversion of the work done by moving the simulation cell boundary on compression (or, equivalently, the Langmuir trough wall in the experiments [21]), the monolayer system possesses a certain amount of excess lattice strain energy (i.e., the energy difference between the rhombohedral and the hexagonal phase). The simulation results discussed in Sec. III A have already demonstrated that the buildup of this lattice strain energy on compression of the monolayer can, eventually, lead to a phase transition if the excess strain energy exceeds the energy barrier between the rhombohedral and the resulting hexagonal phase. As the excess strain energy is released, the monolayer relaxes into a local equilibrium configuration. Now, the purpose of creating a vacancy in the monolayer is to introduce an energy perturbation to the system. If the monolayer is already on the brink of a phase transition, any small energy perturbation will trigger the phase transition. As was shown in Fig. 8, at the coverage of 0.3 (for a hexagonal

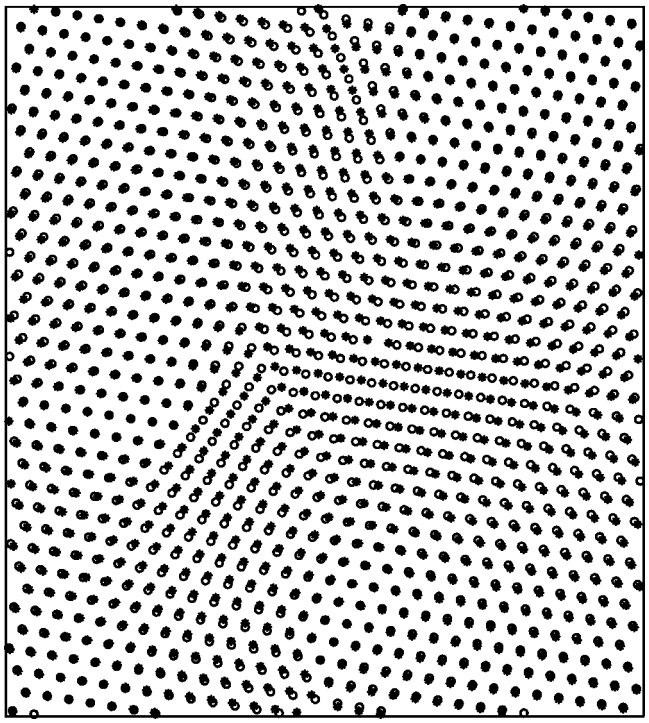

FIG. 11. Initial configuration (empty circles) of the monolayer containing a vacancy at a coverage of 0.4 and final configuration (stars) after the isothermal relaxation.

structure) the presence of a vacancy only gives rise to a local particle relaxation, while at the coverage of 0.35 (for a rhombohedral structure) the vacancy triggers the phase transition (cf. Fig. 9). Since imperfect hexagonal structures contain even more lattice strain energy (at the same coverage), the particles have a high propensity to rearrange in order to form a more stable configuration. In addition, the results described in this section show that the presence of vacancies can trigger such phase transitions at even lower coverages.

Finally, we note again that the calculations presented here were carried out for a relatively large ratio of the potential to kinetic energy of the particles (of 3.77×10^6), which facilitates the MD simulations in terms of the CPU time required to achieve equilibration. A system with such a high ratio of potential to kinetic energy is crystalline [26]. We have repeated the calculations for lower ratios, and have found that the main results described in this paper are essentially unchanged, although their magnitudes (in particular, with respect to the large-scale particle rearrangements) are greatly reduced. This can be easily understood since, for lower ratios of the potential to kinetic energy, the interactions between the particles are weaker.

IV. CONCLUSIONS

Molecular dynamics simulations of the compression of colloidal monolayers at the oil-water interface have been performed in order to investigate the occurrence of solid-to-solid phase transitions and the role that defects play with regard to the stability of the monolayers. It was found that the compression of the monolayers has ''healing'' effects on

imperfections in the monolayers, i.e., initial defects vanish rapidly as the compression proceeds. The MD simulations also showed that an anisotropically compressed monolayer undergoes a sequence of hexagonal-to-rhombohedral-to-hexagonal phase transitions. The number of defects has a direct influence on the occurrence of these phase transitions, e.g., phase transitions from hexagonal to rhombohedral packing are less likely to occur if the monolayers abound with defects (in which case the lattice spacings are more likely to reduce isotropically). However, when a monolayer has relatively few defects, it was found that transitions from hexagonal to rhombohedral packing occur readily under compression. Recently, such solid-to-solid phase transitions were also observed in the compression of antibody monolayers (e.g., monolayers of immunoglobulin G macromolecules at the air-water interface [27]), which can be employed to study the surface activity and unfolding of proteins [28].

Next, a vacancy was created in an otherwise perfect monolayer in order to introduce an energy perturbation. Here it was found that the vacancy can persist in a hexagonal lattice. However, if the strain energy of a rhombohedral lattice is sufficiently large, the vacancy formation can lead to a rearrangement of the particles and the concomitant expulsion of the vacancy.

Recently, there has been increased interest in the investigation of the diffusion of point defects in two-dimensional colloidal crystals [25]. In *three-dimensional* systems, diffusion is thought to occur via sequential, single-particle hopping mechanisms (e.g., direct exchange, monovacancy, interstitial, interstitialcy, divacancy mechanisms, etc. [29]). However, the present results would indicate that in strained *two-dimensional* systems, diffusion can also occur via the collective motion of many particles. Although one has to be careful in generalizing results to higher dimensions [30], it is conceivable that the generic features of the two-dimensional diffusion mechanisms found in the present work may also apply to three dimensions. This would be particularly significant for low-dimensional semiconductor devices fabricated by nonequilibrium growth techniques (such as molecular beam epitaxy).

[1] R.J. Hunter, *Introduction to Modern Colloid Science* (Oxford University Press, Oxford, 1993).

[2] J. Lyklema, *Fundamentals of Interface and Colloid Science* (Academic, London, 1991).

[3] J.C. Earnshaw and D.J. Robinson, J. Phys.: Condens. Matter **2**, 9199 (1990).

[4] R. Aveyard and J.H. Clint, J. Chem. Soc., Faraday Trans. **91**, 2681 (1995); **92**, 85 (1996).

[5] R. Aveyard, P. Cooper, P.D.I. Fletcher, and C.E. Rutherford, Langmuir **9**, 604 (1993).

[6] R. Aveyard, J.H. Clint, and D. Nees, Colloid Polym. Sci. **278**, 155 (2000).

[7] R.K. Kalia and P. Vashishta, J. Phys. C **14**, L643 (1981).

[8] D. Frenkel and J.P. McTague, Phys. Rev. Lett. **42**, 1632 (1979).

[9] S. Toxvaerd, Phys. Rev. Lett. **44**, 1002 (1980).

[10] A.J. Armstrong, R.C. Mockler, and W.J. O'Sullivan, J. Phys.: Condens. Matter **1**, 1707 (1989).

[11] R. Zangi and S.A. Rice, Phys. Rev. E **58**, 7529 (1998).

[12] T. Terao and T. Nakayama, Phys. Rev. E **60**, 7157 (1999).

[13] P. Pieranski, Phys. Rev. Lett. **45**, 569 (1980).

[14] J.M. Kosterlitz and D.J. Thouless, J. Phys. C **5**, L124 (1972); **6**, 1181 (1973).

[15] B.I. Halperin and D.R. Nelson, Phys. Rev. Lett. **41**, 121 (1978); D.R. Nelson and B.I. Halperin, Phys. Rev. B **19**, 2457 (1979).

[16] A.P. Young, Phys. Rev. B **19**, 1855 (1979).

[17] A.H. Marcus and S.A. Rice, Phys. Rev. E **55**, 637 (1997).

[18] R. Aveyard, J.H. Clint, D. Nees, and V.N. Paunov, Langmuir **16**, 1969 (2000).

[19] J. Sun and T. Stirner, Langmuir **17**, 3103 (2001).

[20] M. P. Allen and D. J. Tildesley, *Computer Simulation of Liquids* (Clarendon Press, Oxford, 1992).

[21] R. Aveyard, J.H. Clint, D. Nees, and N. Quirke, Langmuir **16**, 8820 (2000).

[22] D.S. Fisher, B.I. Halperin, and R. Morf, Phys. Rev. B **20**, 4692 (1979).

[23] E. Cockayne and V. Elser, Phys. Rev. B **43**, 623 (1991).

[24] E. Frey, D.R. Nelson, and D.S. Fisher, Phys. Rev. B **49**, 9723 (1994).

[25] A. Pertsinidis and X.S. Ling, Nature (London) **413**, 147 (2001).

[26] C.C. Grimes, Surf. Sci. **78**, 379 (1978).

[27] R.L. Kayushina, Yu. Khurgin, G. Sukhorukov, and T. Dubrovsky, Physica B **198**, 131 (1994).

[28] A. Tronin, T. Dubrovsky, S. Dubrovskaya, G. Radicchi, and C. Nicolini, Langmuir **12**, 3272 (1996).

[29] *Diffusion in Crystalline Solids*, edited by G. E. Murch and A. S. Nowick (Academic, London, 1984).

[30] R. Peierls, *Surprises in Theoretical Physics* (Princeton University Press, Princeton, 1979), Chap. 4.1.